

Isolation of Rhenium and ReO_x Species within ZSM5 Channels and their Catalytic Function in the Activation of Alkanes and Alkanols

Howard S. Lacheen, Paul J. Cordeiro, and Enrique Iglesia*^[a]

Abstract: Synthesis protocols, structures, and reactivity of Re-oxo species grafted onto H-ZSM5, and their subsequent conversion to Re-clusters through contact with H_2 or CH_4 were studied by using Raman, infrared, and X-ray absorption spectroscopies. Reactivity measurements by using alkane and alkanol reactants were also examined. Sublimation of Re_2O_7 at 723 K led to a stoichiometric exchange with each ReO_x species replacing one proton. Raman features for Re_2O_7 disappeared during thermal treatment and Raman bands assigned to distorted-tetrahedral $\text{Si-O}_f\text{ReO}_3\text{-Al}$ (O_f : zeolite-lattice oxygen atoms) species emerged; infrared bands for acidic OH groups in H-ZSM5 weakened concurrently. X-ray absorption near-edge and fine-structure spectra detected the formation of distorted-tetrahedral Re^{7+} -oxo species during thermal treatment of $\text{Re}_2\text{O}_7/\text{H-ZSM5}$ mixtures in air, and

their subsequent reduction to Re^0 in H_2 or CH_4 to form encapsulated Re metal clusters similar in diameter ($\approx 8 \text{ \AA}$) to the channel intersections in ZSM5. $\text{Si-O}_f\text{ReO}_3\text{-Al}$ species in $\text{ReO}_x\text{-ZSM5}$ catalyzed the oxidative conversion of $\text{C}_2\text{H}_5\text{OH}$ to acetaldehyde, acetal, and ethyl acetate with very low selectivity to CO_x ($< 1\%$). Unprecedented turnover rates were exhibited at temperatures much lower than previously found for ReO_x -based catalysts, and without deactivation or sublimation processes ubiquitous in crystalline Re^{7+} compounds at temperatures required for catalysis. Encapsulated Re metal clusters formed by the reduction of $\text{Si-O}_f\text{ReO}_3\text{-Al}$ precursors led to CH_4 pyrolysis and C_3H_8 dehydrocyclodimeri-

zation rates (per Re) that are higher than those previously reported for zeolite-based catalysts. The rate of CH_4 conversion to benzene, by using Re-ZSM5 , was $\approx 30\%$ higher than that of the best reported catalysts, based on encapsulated MoC_x clusters, whereas C_2H_4 and C_{6+} arene selectivities were similar. C_3H_8 activity and selectivity of Re-ZSM5 was significantly higher than that of Ga-ZSM5 , the best reported catalyst for these reactions. Reaction rates (per Re) were independent of the Re/Al_f (Al_f : aluminum framework) ratio for both Re and ReO_x species. This is consistent with the uniform character of the structures formed during grafting of the ReO_x species through sublimation and their ability to retain their homogeneity even after their reduction to encapsulated Re-clusters.

Keywords: ethanol • oxidation • methane • propane • rhenium • zeolites

Introduction

Supported rhenium-based materials have received limited attention as oxidation catalysts, in spite of their high reactivity in epoxidation and metathesis catalysis as organometallic complexes,^[1–3] because of the highly volatile nature of Re-oxo species. Recently, zeolites were reported as useful scaffolds for Re complexes and clusters, but the location and

local structure of Re species remain uncertain.^[4–11] Re nitrides within zeolite channels have been prepared by Iwasa and co-workers by means of grafting methyl Re trioxide (MTO) to a zeolite and then reacting with NH_3 ,^[6–8] these materials catalyze benzene reactions with O_2 to form phenol.^[5] Re-clusters in ZSM5 catalysts have been prepared by impregnation of H-ZSM5 with NH_4ReO_4 and treatment in H_2 to give active catalysts for pyrolysis of $\text{C}_1\text{–C}_4$ alkanes.^[4,9,10,12,13]

We recently reported the vapor-phase exchange of Re_2O_7 (sublimes at 535 K; 100 Pa $\text{Re}_2\text{O}_7(\text{g})$ at 496 K)^[14,15] with H-ZSM5.^[16] Similar methods were previously used to graft $(\text{Mo}_2\text{O}_5)^{2+}$ species prepared from MoO_3 ^[17,18] (sublimes at 1425 K, 4.9 Pa at 973 K).^[15] These protocols led to uniform and highly-dispersed Re^{7+} -oxo species that were amenable

[a] Dr. H. S. Lacheen, P. J. Cordeiro, Prof. E. Iglesia
Department of Chemical Engineering
University of California at Berkeley
Berkeley, CA 94720 (USA)
Fax: (+1) 510-642-4778
E-mail: iglesias@chem.berkeley.edu

to spectroscopic assessment of their coordination, chemical environment, and oxidation state. The structure and function of the Re^{7+} -ZSM5 catalysts were independent of their Re content. Moreover, strong interactions between Re-oxo monomers and framework Al sites (Al_f) led to stable structures at temperatures well above those that would normally cause loss of Re_2O_7 domains by sublimation onto mesoporous supports.^[19] The nonoxidative C_3H_8 conversion rates of Re-clusters dispersed on H-ZSM5 are reported here to be independent of Re content and higher than that of Ga-ZSM5, the best catalyst reported previously for these reactions.^[20,21] Finally, we show that isolation of Re-oxides on zeolites leads to catalysts, suitable for oxidation of $\text{C}_2\text{H}_5\text{OH}$ to $\text{CH}_3\text{CH}_2\text{OCOCH}_3$ (ethyl acetate) and $(\text{CH}_3\text{CH}_2\text{O})_2\text{-CHCH}_3$ (acetal) at near ambient temperatures, that display unprecedented reactivity and selectivity.

Results and Discussion

Raman spectroscopy of $\text{Re}_2\text{O}_7/\text{H-ZSM5}$ mixtures: Raman spectra of aqueous NH_4ReO_4 and of $\text{Re}_2\text{O}_7/\text{H-ZSM5}$ catalysts before and after thermal treatment at 823 K are shown in Figure 1. Crystalline Re_2O_7 , shown in Figure 1 as a mix-

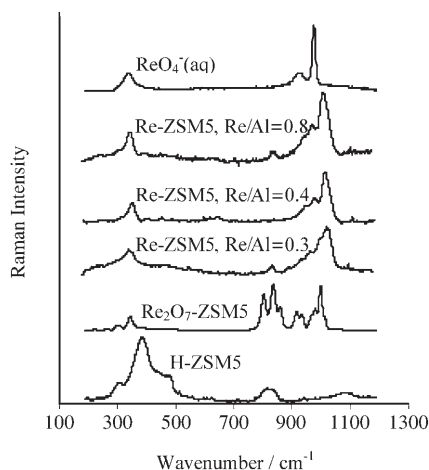


Figure 1. Raman spectra of $\text{Re}_2\text{O}_7/\text{H-ZSM5}$ and reference compound aqueous NH_4ReO_4 . At 298 K, the H-ZSM5 zeolites were exposed to UV light before being mixed with Re_2O_7 . $\text{Re}_2\text{O}_7/\text{H-ZSM5}$ was heated at 823 K in a Raman cell in dry air, then cooled to ambient temperature before measurements were taken. The Raman cell was rotated at 7 Hz.

ture with H-ZSM5, exhibits Re=O modes for tetrahedral Re-oxo species near $\tilde{\nu}=1000\text{ cm}^{-1}$, Re=O modes for octahedral Re-oxo species near $\tilde{\nu}=800\text{ cm}^{-1}$, and weaker O-Re-O modes near $\tilde{\nu}=300\text{ cm}^{-1}$.^[22,23] ReO_4^- anions in aqueous NH_4ReO_4 exhibit tetrahedral symmetry,^[24,25] and Raman bands at $\tilde{\nu}=970, 921,$ and 332 cm^{-1} that are assigned to $A_1, E,$ and T_1 modes, respectively (Table 1). The Re^{7+} centers in solid NH_4ReO_4 are distorted from perfect T_d symmetry, and as a result, the doubly degenerate E band (T_d symmetry) is split into two bands.^[26-29]

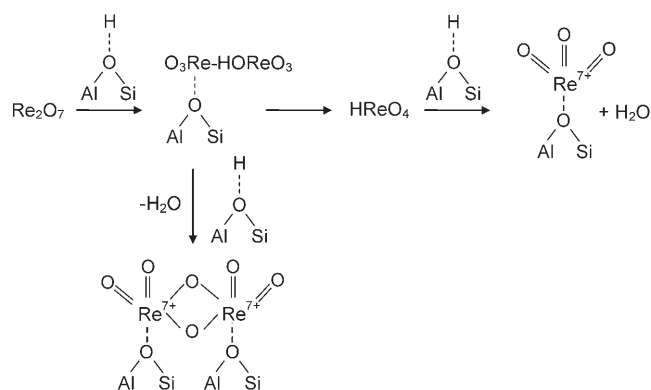
Table 1. Raman shifts for Re standard compounds and exchanged Re-ZSM5 materials.^[a]

Sample	Raman shift [cm^{-1}] this study	Raman shift [cm^{-1}] previous studies	Stretch	Ref.
ReO_4^-	970	970	$\nu_s\text{Re-O}$	[25]
	921	916	$\nu_{as}\text{Re-O}$	
	332	332	O-Re-O	
NH_4ReO_4	966	965	$\nu_s\text{Re-O}$	[27]
	915, 893	911, 890	$\nu_{as}\text{Re-O}$	
	338	339, 332	O-Re-O	
Re_2O_7	994, 976, 968, 930, 912	993, 975, 960, 925, 905	Re-O (T_d)	[23]
	855, 830, 798	854, 831, 798	Re-O (O_h)	
	341, 299, 170	339, 298, 166	Re-O-Re	
Re-ZSM5 dry air ^[b]	1020		$\nu_s\text{Re-O}$	
	980		$\nu_{as}\text{Re-O}$	
	347		O-Re-O	
Re-ZSM5 wet air ^[c]	975		$\nu_s\text{Re-O}$	
	941		$\nu_{as}\text{Re-O}$	
	334		O-Re-O	

[a] Re-ZSM5 was treated at 823 K in a Raman cell in dry air, then cooled to room temperature before measurements were taken. Re-ZSM5 was then rehydrated by passing dry air through a bubbler at 298 K. [b] Re/Al=0.4, 823 K. [c] Re/Al=0.4, 298 K.

The Raman spectra show bands at $\tilde{\nu}=1020, 980,$ and 347 cm^{-1} if the $\text{Re}_2\text{O}_7/\text{H-ZSM5}$ physical mixtures (Re/Al_f=0.4) were treated in dry air at 823 K (Figure 1); these bands are indicative of distorted-tetrahedral ReO_4^- structures, but have spectral features that are shifted to higher frequencies relative to those of aqueous ReO_4^- and NH_4ReO_4 compounds. These thermal treatments led to the transformation of crystalline Re_2O_7 into a dispersed Re-oxo species, ostensibly grafted at exchange sites in H-ZSM5. The Raman spectra of $\text{Re}_2\text{O}_7/\text{H-ZSM5}$ treated at 823 K in dry air show bands that have been assigned to A_1 ($\tilde{\nu}=1020\text{ cm}^{-1}$), E ($\tilde{\nu}=980\text{ cm}^{-1}$), and T_1 ($\tilde{\nu}=347\text{ cm}^{-1}$) modes, analogous to the assignments of similar bands in aqueous ReO_4^- ions.^[24,25] The A_1 vibrational mode is the symmetric Re-O stretch, E is the antisymmetric stretch, and T_1 is the O-Re-O bending mode. These spectra are consistent with distorted-tetrahedral Re-oxo species present as isolated Si-O_fReO₃-Al species connected to the aluminum framework (Al_f) through zeolite-lattice oxygen atoms (O_f).

Reactions of vapor-phase Re_2O_7 with $\text{Al-O}_f\text{H-Si}$ can lead to $\text{O}_3\text{Re-(OH)ReO}_3$ species (Scheme 1), which can then react either with a vicinal proton to form $\text{O}_2\text{Re}(\mu\text{-O})_2\text{ReO}_2^{2+}$ dimers or cleave a Re-O bond to form HReO_4 (perrhenic acid, b.p. 500 K^[15]). HReO_4 is more volatile than Re_2O_7 (b.p. 633 K^[14]) and in its gaseous state subsequently reacts with nonvicinal protons to form a grafted Si-O_fReO₃-Al monomer with the concurrent formation of a H_2O molecule. Raman spectroscopy did not detect dimer structures, which are expected to exhibit $\mu\text{-O}$ bands at $\tilde{\nu}=450$ and 180 cm^{-1} ,^[23] the absence of Re-O-Re bands may reflect, however, nonuniform dimer structures, for which the



Scheme 1. Proposed exchange pathways for the reaction between vapor-phase Re_2O_7 and H-ZSM5.

structural nonuniformity is imposed by the distribution of distances between Al sites prevalent within ZSM5 frameworks.

$\text{Re}_2\text{O}_7/\text{H-ZSM5}$ mixtures with Re/Al_f ratios of 0.3 and 0.8 (Figure 1) showed the same three Raman bands as samples with intermediate Re/Al_f ratios (0.4) after treatment in dry air at 823 K. Therefore, the structure of the grafted Re-oxo species is independent of the degree of exchange. A small shoulder, detectable only in the sample containing a Re/Al_f ratio of 0.3, appears near the symmetric Re-O stretch at $\tilde{\nu}=1000\text{ cm}^{-1}$, possibly as a result of a small fraction of the grafted Re-oxo species interacting with silanols at external surfaces or with extraframework Al within channels.

After exposure of the sample to a 20% O_2/He stream saturated with H_2O at 298 K, the Raman spectral features of Re-ZSM5 are shifted to lower frequencies. Water is expected to decrease Raman frequencies for accessible ReO_x species as a result of an increase in Re coordination;^[28] these interactions cannot occur in crystalline NH_4ReO_4 as most of the Re centers are inaccessible to gaseous H_2O . For Re-ZSM5 with $\text{Re}/\text{Al}_f=0.4$, this treatment shifted the $\tilde{\nu}=1020\text{ cm}^{-1}$ band for the symmetric Re-O stretch to 975 cm^{-1} , the antisymmetric mode from $\tilde{\nu}=980$ to 941 cm^{-1} , and the O-Re-O bending mode from $\tilde{\nu}=347$ to 334 cm^{-1} (Table 1).^[30] These shifts confirmed the exclusive presence of accessible tetrahedral structures, which are distorted by coordination with H_2O . The band for O-Re-O stretches at $\tilde{\nu}=347\text{ cm}^{-1}$ was affected only weakly by interactions with H_2O , evidently the O-Re-O bending modes are insensitive to local coordination, a conclusion confirmed by similar frequencies shown for O-Re-O bands ($\tilde{\nu}=332\text{--}341\text{ cm}^{-1}$) measured for all reference Re-oxo compounds, irrespective of their Re coordination symmetry (Table 1).

Infrared spectra of $\text{Re}_2\text{O}_7/\text{H-ZSM5}$: The infrared spectra for $\text{Re}_2\text{O}_7/\text{H-ZSM5}$ physical mixtures treated in dry air at 723 K for Re/Al_f ratios between 0 and 0.44 are shown in Figure 2. Acidic hydroxyl groups ($\text{Si-O}_f\text{H-Al}$ at $\tilde{\nu}=3600\text{ cm}^{-1}$) and traces of silanol groups ($\text{Si-O}_f\text{H}$ at $\tilde{\nu}=3740\text{ cm}^{-1}$) are evident in the spectra of H-ZSM5. The $\text{Si-O}_f\text{H-Al}$ band intensity decreased linearly as the Re/Al ratio

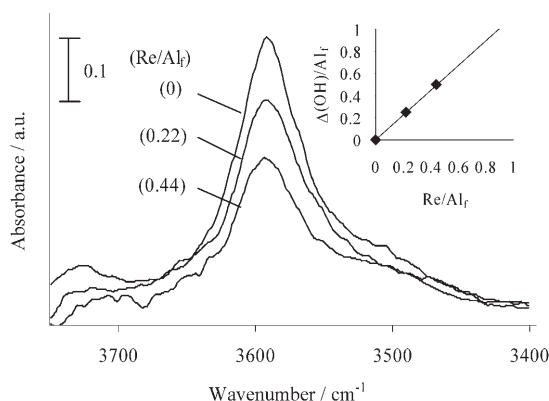


Figure 2. Infrared spectra of $\text{ReO}_x\text{-ZSM5}$ ($0 < \text{Re}/\text{Al}_f < 0.44$). The insert shows the loss of acidic hydroxyls, $\Delta(\text{OH})/\text{Al}_f$, versus Re/Al_f . The change in hydroxyl intensity, $\Delta(\text{OH})/\text{Al}_f$, was measured by using infrared spectroscopy from the difference between the area of the peak centered at $\tilde{\nu}=3600\text{ cm}^{-1}$ for exchanged samples and the normalized peak of unexchanged H-ZSM5 ($\text{Re}/\text{Al}_f=0$). ZSM5 bands between $\tilde{\nu}=1750$ and 2100 cm^{-1} were used as internal standards to correct for differences in sample thickness and ZSM5 concentration.

increased (inset, Figure 2), consistent with each Re-oxo species replacing one H^+ ($\Delta(\text{OH})/\text{Re}=1.1 \pm 0.1$). The $\text{Si-O}_f\text{H}$ band intensity also decreased as the Re content increased, a result of the $\text{O}_3\text{Si-ReO}_3$ species that forms at external surfaces and accounts for $\approx 10\%$ of all Re atoms.^[31] The presence of both Re-oxo monomers and dimers (Scheme 1) would lead to the observed exchange stoichiometry (≈ 1) at $\text{Si-O}_f\text{H-Al}$ sites, whereas the Raman bands observed for Re-ZSM5 suggest that the Re-oxo species have the distorted-tetrahedral coordination characteristic of $\text{Si-O}_f\text{ReO}_3\text{-Al}$ monomers (Scheme 1), instead of the higher local coordination expected of Re-oxo dimers. Below, we provide additional evidence for the structure and oxidation state of Re centers and for their single-site nature and uniform coordination based on the dynamics of their reduction in H_2 and their X-ray absorption near-edge fine-structure (XANES) spectra.

Treatment of $\text{Re}_2\text{O}_7/\text{H-ZSM5}$ samples in dihydrogen: H_2 consumption rates as a function of temperature for Re-ZSM5 samples with Re/Al_f ratios between 0 and 0.44 are shown in Figure 3. Maximum reduction rates were observed at 600–615 K in all samples, although crystalline Re_2O_7 powders showed a maximum reduction rate at 565 K. The initial reduction temperatures (530 K) are also similar for all three samples, consistent with the lack of influence of the Re content on the Raman spectra and exchange stoichiometry. The sample that had the highest loading ($\text{Re}/\text{Al}_f=0.44$) showed a reduction profile different from the samples that had a lower Re content, apparently as a result of the concurrent formation of larger ReO_x aggregates during H_2 treatment, evidence for which is presented below.

The amounts of H_2 consumed and of H_2O formed given in Table 2 were calculated by using the reduction rate profiles seen in Figure 3. The reduction of $\text{Re}_2\text{O}_7/\text{H-ZSM5}$

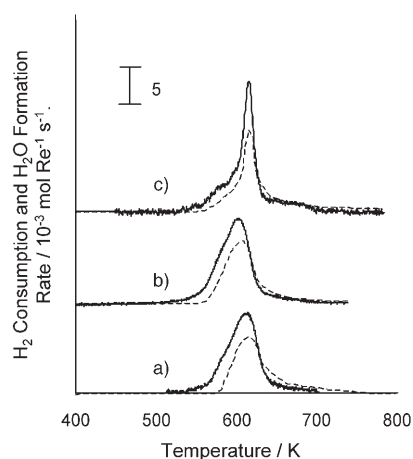


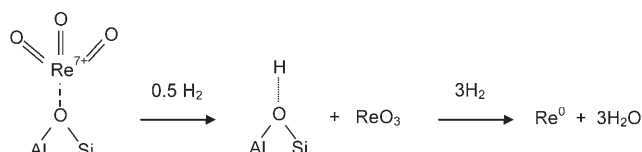
Figure 3. Temperature programmed reduction of $\text{Re}_2\text{O}_7/\text{H-ZSM5}$ in H_2/He (4 kPa) with Re/Al_f ratios; a) 0.08, b) 0.22, and c) 0.44. $\text{Re}_2\text{O}_7/\text{H-ZSM5}$ samples were heated to 723 K in dry air for 1 h prior to reduction. Heating rate was 0.17 K s^{-1} . H_2 consumption (—), H_2O production (----).

Table 2. Reduction stoichiometry of Re-ZSM5 .^[a]

Re/Al_f	H_2/Re consumed	$\text{H}_2\text{O}/\text{Re}$ formed
0.08	3.3	2.8
0.22	3.5	3.0
0.44	3.4	2.7

[a] Samples (0.05–0.2 g), in H_2 (5 kPa) and He (96 kPa), with a flow rate of $1 \text{ cm}^3 \text{ s}^{-1}$, 298–723 K (0.17 K min^{-1}).

treated at 773 K consumed 3.4 ± 0.1 H_2 molecules per Re atom, indicative of the stoichiometric reduction of all Re^{7+} atoms in each sample to Re^0 . However, only 2.8 ± 0.1 H_2O molecules per Re atom were formed as H_2 was used to replace the reduced Re-oxo cations with H^+ at exchange sites. The difference between the amounts of H_2 consumed and the amount of H_2O formed was 0.5 ± 0.1 H_2 molecules per Re atom for all samples, consistent with either $\text{Si-O}_f\text{ReO}_3\text{-Al}$ monomers at one exchange site or $\text{O}_2\text{ReO}_2\text{ReO}_2^{2+}$ dimers interacting with two exchange sites, although not with the reduction of ungrafted Re_2O_7 domains or with the presence of unreducible Re-oxo species. The consumption of H_2 without concurrent H_2O evolution at lower temperatures suggests that $\text{Si-O}_f\text{ReO}_3\text{-Al}$ is first detached from exchange sites to form a ReO_3 species, which is then reduced to form Re^0 , and equimolar amounts of H_2 are consumed and H_2O is produced (Scheme 2). We cannot exclude, however, that the temporal shift between H_2 con-



Scheme 2. Stepwise reduction of $\text{Si-O}_f\text{ReO}_3\text{-Al}$ monomers.

sumption and H_2O evolution may merely reflect a slight chromatographic retention of H_2O as it forms.

X-ray absorption spectra during thermal treatment in air or dihydrogen: X-ray absorption near-edge structure (XANES) and extended X-ray absorption fine-structure (EXAFS) spectra were measured at the Re L_I -edge and L_{III} -edge. Figure 4 shows the Re L_I -near-edge spectra (12.527 keV

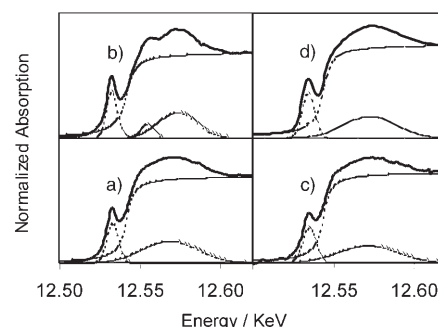


Figure 4. Re L_I -edge XANES recorded at 298 K for a) Re_2O_7 , b) NH_4ReO_4 , c) $\text{Re}_2\text{O}_7/\text{H-ZSM5}$ physical mixture at 298 K, and d) $\text{Re}_2\text{O}_7/\text{H-ZSM5}$ after treatment at 773 K in dry air. Spectral deconvolution was performed by using a least-squares fit, 1 arctangent and 2-3 Gaussian functions.

edge for Re^0) for $\text{Re}_2\text{O}_7/\text{H-ZSM5}$ ($\text{Re}/\text{Al}_f=0.22$) and for crystalline compounds that have known structures. All spectra showed a pre-edge feature, caused by transitions of Re electrons from the 2s orbital into empty d orbitals; these transitions are dipole-forbidden in centrosymmetric structures, but become allowed as a result of orbital hybridization as the initial octahedral symmetry is distorted. Pre-edge intensities listed in Table 3 were calculated by using regression

Table 3. Re L_I -edge pre-edge intensity determined by deconvolution of near-edge spectra between -80 and 100 eV (relative to Re^0 edge, 12.527 keV) by using 2-3 Gaussian and 1 arctangent functions.

Sample	Pre-edge peak		
	fwhm ^[a] [eV]	Height ^[b]	Intensity ^[b,c]
Re_2O_7	10.1	0.44	4.4
NH_4ReO_4	9.20	0.52	4.8
$\text{Re}_2\text{O}_7/\text{H-ZSM5}$ ($\text{Re}/\text{Al}_f=0.22$)			
298 K, dry air	11.3	0.39	4.4
723 K, dry air	10.2	0.50	5.1

[a] Full-width at half-height of maximum. [b] Arbitrary units. [c] Intensity = fwhm \times height.

methods described in the Experimental Section. Distorted tetrahedral Re centers in NH_4ReO_4 gave a pre-edge feature that has an intensity of 4.8 ± 0.1 , although Re_2O_7 , which has equimolar tetrahedral and octahedral centers,^[22] gave weaker pre-edge features (4.4 ± 0.1); this latter value is larger than expected from the number of tetrahedral Re centers in Re_2O_7 , because octahedral Re centers are also se-

verely distorted in crystalline Re_2O_7 .^[22] Physical mixtures of Re_2O_7 and H-ZSM5 retained all the spectral features of crystalline Re_2O_7 and a pre-edge intensity of 4.3 ± 0.1 in dry air until treated at 723 K. Consequently, the pre-edge intensity increased to 5.1 ± 0.1 ; indicative of an increase in the tetrahedral character of Re^{7+} centers. This evolution in spectral features is consistent with the formation of noncentrosymmetric structures on zeolitic surfaces during thermal treatment in air and occurs in the same temperature range as the changes in the infrared and Raman spectral features implicated in exchange.

The Re L_{III} -edge was used to confirm the heptavalent nature of the Re centers and the dynamics of their reduction to Re metal clusters in Re-ZSM5. Overlap of spectral regions for Re L_{II} - and L_{I} -edges (11.96 and 12.527 keV, respectively) make these measurements inaccurate if L_{I} -edges are used. The spectrum for $\text{Re}_2\text{O}_7/\text{H-ZSM5}$ physical mixtures ($\text{Re}/\text{Al}_f=0.22$) treated in air at 723 K is shown in Figure 5.

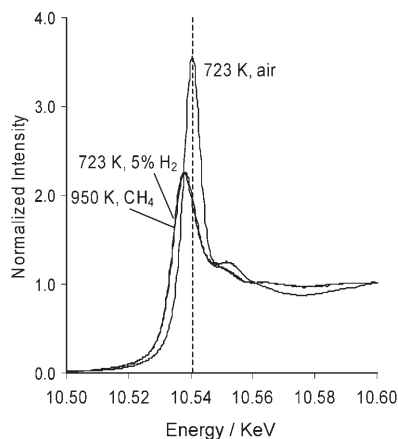


Figure 5. Re L_{III} -edge XANES spectra recorded at 298 K for $\text{Re}_2\text{O}_7/\text{H-ZSM5}$ after thermal treatment in dry air at 723 K, treatment in H_2/He (5 kPa) at 723 K, and treatment in CH_4/Ar (91 kPa) at 950 K.

The white line at 10.54 keV in $\text{Re}_2\text{O}_7/\text{H-ZSM5}$ at 723 K in air, arising from $2p_{3/2} \rightarrow 5d_{3/2}$ (or $5d_{5/2}$) transitions, weakened and shifted to lower energies during exposure to H_2 (5 kPa) at 723 K. Near-edge spectra were fitted as linear combinations of the spectra for the starting material ($\text{Re}_2\text{O}_7/\text{H-ZSM5}$ at 723 K in dry air) and for each sample after treatment in H_2 at 723 K to measure the extent of reduction; these results are shown in Figure 6, together with values obtained independently from the H_2 consumption rates during similar treatments. In both cases, reduction was first detected at ≈ 500 K and was complete by ≈ 700 K. After H_2 treatment at 723 K, samples were exposed to He at 950 K and then to CH_4 at 950 K (90 kPa; conditions typical of CH_4 pyrolysis reactions^[4,9,10]). Re L_{III} -edge spectra were unaffected by exposure of the sample to CH_4 at 950 K, which indicated that no further reduction had occurred.

The L_{III} -edge k^3 -weighted Fourier-transform of the extended fine-structure (FT-EXAFS) for $\text{Re}_2\text{O}_7/\text{H-ZSM5}$

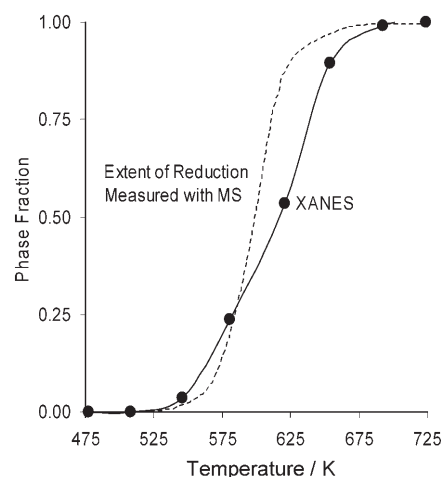


Figure 6. Linear combination fit of the L_{III} -edge XANES spectra of Re-ZSM5 during reduction in H_2/He (\bullet). The extent of reduction measured by using mass spectrometry during reduction in H_2/He (4 kPa) is also shown (\circ).

heated in dry air to 723 K at 0.17 K s^{-1} ($\text{Re}/\text{Al}_f=0.22$) is shown in Figure 7. The feature at 1.4 \AA represents scattering of an ejected electron by a neighboring atom;^[32] the true

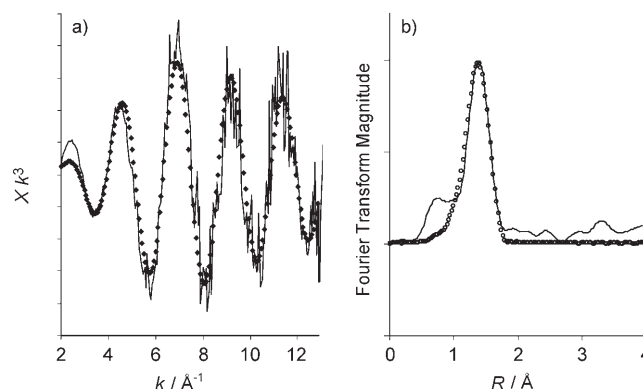


Figure 7. a) Re L_{III} -edge k^3 -weighted EXAFS spectra of Re-ZSM5 ($\text{Re}/\text{Al}_f=0.22$) after thermal treatment at 723 K in dry air: experimental data (—) and simulation data (\blacklozenge). b) the Fourier transform of the EXAFS spectra: experimental data (—) and simulation data (\circ).

radial position of the neighboring atom will lie at a slightly larger distance (by $\approx 0.2 \text{ \AA}$), which can be estimated from compounds with known Re-O bond lengths. Preliminary fine-structure spectra, and phase-shift and amplitude functions were simulated by using NH_4ReO_4 as the model (Re-O distances of 1.71 \AA and a coordination number of four). The EXAFS and FT-EXAFS k^3 -weighted spectral fits are given in Figure 7. A fit of the Re-ZSM5 EXAFS spectra gave oxygen coordination of 1 and 3 at 1.8 and 1.7 \AA (Table 4), respectively, consistent with $\text{Al-O}_f\text{ReO}_3\text{-Si}$ grafted onto exchange sites (Scheme 1). A second-shell Re center was not detected, although this alone is not compelling evidence for a monomeric species, as long-range scattering is

Table 4. Re L_{III} -edge k^3 -weighted EXAFS spectra fitting parameters for Re-ZSM5.

Sample ^[a] [10^{-3} \AA^2]	Shell	CN ^[b]	R [\AA] ^[c]	ΔE [eV] ^[d]	$\Delta(\sigma^2)$ ^[e]
723 K, 20% O_2/He ^[f,g]	Re-O	3	1.7	0.43	-0.7
	Re-O	1	1.8	0.63	-1.7
723 K, 5% H_2	Re-Re	5.9	2.8	0.8	1.2
950 K, CH_4	Re-Re	6.0	2.8	-0.9	2.8
simulated Re^0 cluster ^[h]	Re-Re	5.5	2.8	-	-

[a] All spectra were recorded at 298 K. [b] Coordination number. [c] Interatomic distance. [d] Edge energy shift. [e] Debye-Waller factor, $\Delta(\sigma^2)$. [f] CNs were fixed. [g] CNs were 3.4 ± 1 and 1.4 ± 1 at 1.8 and 1.7 \AA ($\Delta E_0 = 0.63$ and 0.20 eV), respectively, for $\Delta(\sigma^2)$ fixed at zero. [h] 8.2 \AA in diameter.

weak, and destructive interference may have caused the second-shell contributions of nonvicinal atoms to decrease.

The k^3 -weighted EXAFS spectra for Re-ZSM5 after treatment in H_2 (5 kPa) at 723 K and subsequent exposure to CH_4 at 950 K are shown in Figure 8. The fitting parameters from these k^3 -weighted spectra are shown in Table 4

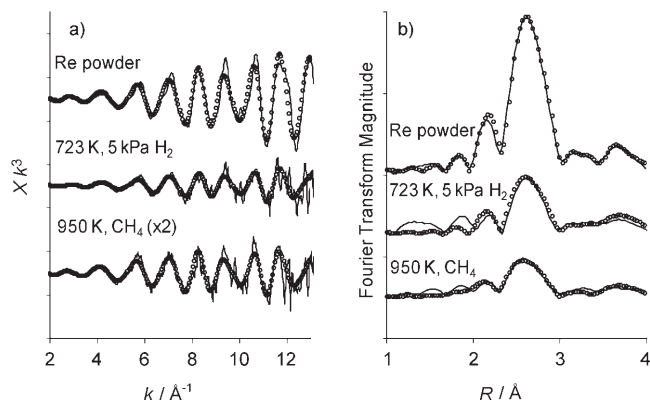


Figure 8. a) Re L_{III} -edge k^3 -weighted EXAFS spectra of Re powder and Re^0 -ZSM5 ($\text{Re}/\text{Al}_f = 0.22$). b) Fourier transform of the EXAFS. Experimental data (—) and simulation data (○).

and the simulated spectra, which overlay the experimental results, are shown in Figure 8. The number of Re nearest-neighbors in Re-ZSM5 is similar, after treatment in H_2 (5.9) or CH_4 (6.0), but smaller than in crystalline Re powder (12). The Re-cluster size inferred from these coordination numbers was unaffected by catalytic CH_4 reactions and similar coordination number values were reported previously by Ichikawa et al.,^[4] in which Re-Re coordination (2.8 \AA) increased from 4.9 to 6.4 during exposure of 5 wt% Re-ZSM5 ($\text{Si}/\text{Al}_f = 20$, $\text{Re}/\text{Al}_f = 0.35$) to CH_4 for 24 h. This remarkable stability of Re-clusters is consistent with the high-melting (3460 K) and Tamman (2300 K) temperatures of Re^0 , and the inhibited coalescence imposed by encapsulation within zeolite channels.^[14]

Re-cluster sizes were estimated by comparing simulated Re-clusters with measured Re-Re coordination numbers. The cluster shown in Figure 9 contains 12 Re atoms around a central Re atom with a Re-Re interatomic distance of

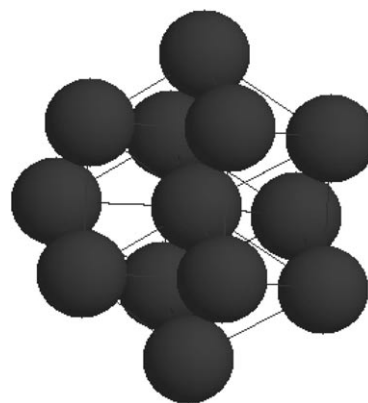


Figure 9. Model Re-cluster containing 13 atoms that was used to simulate Re-MFI EXAFS spectra.

2.8 \AA and a mean coordination number of 5.5 (Table 4). These values are similar, within experimental accuracy, to those estimated from the radial structure function in the Re-ZSM5 ($\text{Re}/\text{Al}_f = 0.22$) sample exposed to CH_4 at 950 K. These simulated clusters give an average diameter of 8.2 \AA , if a Re atomic radius of 1.37 \AA is used^[14,33] and 92% of all Re atoms are exposed at surfaces. The clusters are slightly larger than the predicted sizes for the largest occluded spheres in ZSM5 zeolite structures (MFI framework; 6.3 \AA),^[34] which suggests that some Re-clusters may reside at external surfaces or that intrachannel clusters may lack the spherical symmetry assumed in simulating their diameter from coordination numbers. Previous studies have shown that Mo-oxo and W-oxo species convert to carbides during CH_4 reactions to form carbide clusters of the same diameter as Re-clusters ($\approx 8.5 \text{\AA}$).^[35-37]

The L_I pre-edge intensities and fine-structure X-ray absorption spectra show that Re_2O_7 acquires a distorted-tetrahedral coordination after thermal treatment in dry air at 723 K, consistent with the grafting of volatile Re-oxo species onto exchange sites in H-ZSM5. Raman spectra and reduction dynamics showed that similar Re-oxo structures were present for Re/Al ratios between 0.1 and 0.4 and that each Re atom replaced one H^+ in H-ZSM5. These results are consistent with $\text{Si-O}_f\text{ReO}_3\text{-Al}$ monomers in Re-ZSM5 (Scheme 1) at intrachannel Al_f sites. The reduction of Re-ZSM5 in H_2 to form $\approx 8 \text{\AA}$ Re^0 clusters makes these materials suitable shape-selective catalysts for CH_4 pyrolysis and C_3H_8 dehydrocyclization, as shown previously by Re-ZSM5 samples prepared by impregnation with aqueous NH_4ReO_4 ,^[13,38] a procedure that leads initially to ReO_x clusters at external surfaces. We have applied the catalytic properties of unreduced ReO_x -ZSM5 to ethanol oxidation and of Re-clusters formed by reduction of Re-oxo species in H_2 to nonoxidative reactions of light alkanes.

Oxidative dehydrogenation of ethanol: The oxidation of ethanol was studied by using the ReO_x -ZSM5 samples prepared by the sublimation methods reported here. $\text{C}_2\text{H}_5\text{OH}$ conversions, oxidative-dehydrogenation turnover rates

(ODH rate per Si-O_fReO₃-Al), and product selectivities are shown in Table 5. Si-O_fReO₃-Al cations act as redox-active centers for oxidative dehydrogenation of C₂H₅OH to

Table 5. C₂H₅OH oxidation on Re-ZSM5 at 373 K.^[a]

Catalyst	Conversion [%] ^[b]	ODH rate [10 ⁻³ mol(Re) ⁻¹ s ⁻¹]	DEE ^[c]	Selectivity [%]			
				CH ₃ CHO	EtAc	Acetal	CO ₂
Re-ZSM5 ^[a] (Re/Al _f =0.1)	0.50	2.2	65.7	16.0	2.3	9.2	<1
Re-ZSM5 ^[a] (Re/Al _f =0.4)	0.59	2.3	26.3	51.8	2.1	16.6	<1

[a] Reactant mixture C₂H₅OH (4 kPa), O₂ (9 kPa), N₂ (1 kPa), pressure balanced with He. [b] DEE Free. [c] DEE = diethylether.

CH₃CHO, and the CH₃CHO formed then reacts on acid sites to form (CH₃CH₂O)₂CHCH₃ (acetal) and with Re-oxo species to form CH₃CH₂OCOCH₃ (ethyl acetate).^[39,40] Hydrogen-atom abstraction from ethoxide intermediates using labile oxygen atoms in ReO_x species is expected to control oxidative-dehydrogenation rates, as in oxidative-alkanol dehydrogenation on RuO_x-based catalysts.^[40]

Supported- and bulk-ReO_x species catalyze methanol oxidation, although few studies have reported their properties for ethanol oxidation reactions.^[40,41] Bulk SbOReO₄·2H₂O materials catalyze C₂H₅OH conversion to CH₃CH₂OCOCH₃ and (CH₃CH₂O)₂CHCH₃ at 573 K;^[42] the ReO_x⁺-ZSM5 materials reported here catalyzed this reaction at much lower temperatures (373 K; Table 5). (C₂H₅)₂O selectivities were 66% at low Re content (Re/Al_f=0.1), as a result of rapid bimolecular condensation reactions on residual Brønsted acid sites. These values decreased as the Re/Al_f ratio increased, as acidic protons are increasingly replaced by Re-oxo species. Oxidative-dehydrogenation rates were similar (2.2 × 10⁻³ mol(C₂H₅OH) mol(Re)⁻¹s⁻¹) if Re-ZSM5 materials with Re/Al_f ratios of 0.1 and 0.4 were used, consistent with the similar ReO_x structures and with the single-site nature of these materials. Thus, grafted Si-O_fReO₃-Al species in zeolites show unprecedented reactivity in ethanol oxidation reactions; their high reactivity is not unexpected in view of the high oxidation reactivity of silica-supported Re₂O₇^[41] and polymer-supported CH₃ReO₃.^[43] The stability made possible by the grafting of isolated Re-oxo species eliminates the volatility issues that have precluded the use of Re oxides as practical oxidation catalysts.

Catalytic activation of propane and methane on ZSM5-encapsulated Re metal clusters:

Re-ZSM5 prepared by impregnation with aqueous NH₄ReO₄ has been reported to catalyze C₃H₈ dehydrocyclodimerization reactions.^[13] These reactions proceed by C₃H₈ dehydrogenation to form C₃H₆ intermediates that subsequently undergo secondary oligomerization, cyclization, and dehydrogenation reactions on acid sites to form stable arenes.^[44] Ga^[45] and Zn^[46,47] also increased arene synthesis rates and selectivities if H-ZSM5 is used (Table 6). Re-ZSM5 samples were treated in H₂/He (4 kPa H₂) at 723 K for 1 h before contact with

C₃H₈ (20 kPa) at 773 K. Re-ZSM5 (Re/Al_f=0.08) showed the highest reported C₃H₈ conversion rates (1.7 × 10⁻¹ mol(C₃H₈) mol(Re)⁻¹s⁻¹); these rates are significantly higher than those reported in earlier studies for Re-ZSM5 catalysts prepared by impregnation (0.22 × 10⁻¹ mol(C₃H₈) mol(Re)⁻¹s⁻¹).^[13] These data show that Re/H-ZSM5 materials prepared by using the sublimation protocols reported here lead to Re dispersions much greater than those for

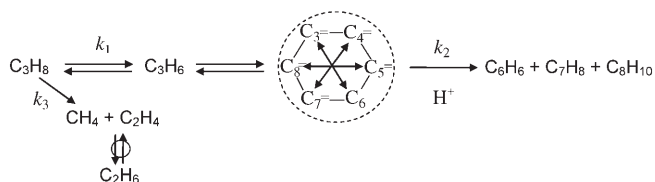
Table 6. C₃H₈ dehydrocyclodimerization rates and product distribution on M-ZSM5 (M = metal; 773 K; 20 kPa C₃H₈). Selectivities are reported for conversions between 10.2 and 11.2%.

Catalyst	M/ Al _f	Initial C ₃ H ₈ turnover rate ^[a]	Selectivity [%]				Ref.
			C ₁ -C ₂	C ₃ =	C ₄ -C ₅	C ₆₊	
Ga ^[b]	0.09	93	28	30	8	34	
Zn ^[c]	0.10	34	- ^[d]	-	-	35	[46]
Re ^[e]	0.08	170	15	60	14	10	
Re ^[f]	0.22	150	6	83	5	5	
Re ^[g]	0.20	22	25	8	-	26	[13]
Re ^[h]	0.44	28	13	72	5	10	

[a] [10⁻³ mol(C₃H₈) mol(M)⁻¹s⁻¹]. [b] C₃H₈ feed rate = 8 cm³g-(catalyst)⁻¹s⁻¹. [c] 778 K, 1 g catalyst, 2000 h⁻¹ GHSV (GHSV = gas hourly space velocity), 10% conversion. [d] Not reported. [e] C₃H₈ feed rate = 16 cm³g-(catalyst)⁻¹s⁻¹. [f] C₃H₈ feed rate = 66 cm³g-(catalyst)⁻¹s⁻¹, 6.7% conversion. [g] C₃H₈ feed rate = 12 cm³min⁻¹, 12.5 kPa, with 0.3 g catalyst, at 823 K, 70% conversion. [h] C₃H₈ feed rate = 15 cm³g-(catalyst)⁻¹s⁻¹, 3.8% conversion.

materials of similar composition prepared by using conventional impregnation methods. The Re/H-ZSM5 catalyst with a Re/Al_f ratio of 0.44 gave lower propane dehydrocyclodimerization rates (0.28 × 10⁻¹ mol(C₃H₈) mol(Re)⁻¹s⁻¹) than samples that have a lower Re content. X-ray diffraction patterns for samples with Re/Al_f ratios above 0.4 showed the presence of some Re metal crystallites (≈100 Å diameter), which were not detected in samples with lower Re/Al_f ratios. No loss in zeolite crystallinity was detected by means of X-ray diffraction after reduction, leading us to conclude that the large Re-clusters formed at high Re loadings (>0.4) reside at external surfaces and lead to larger Re-clusters, consistent with the lower propane reaction rates (per Re) measured on these samples.

To probe the specific effects of Re content on selectivities first-order rate constants for individual reaction steps involved in C₃H₈ conversion to arenes were measured and compared with previously reported reaction networks (Scheme 3^[44] and Table 6). C₃H₈ dehydrogenation (*k*₁) and C₃H₆ cyclodimerization (*k*₂) rate constants are shown in Table 7. The *k*₁ value of Re⁰-ZSM5 (1.1 L mol(Al_f)⁻¹s⁻¹) is more than twice that for Ga-ZSM5 (0.42 L mol(Al_f)⁻¹s⁻¹) at similar M/Al_f ratios. The *k*₁/*k*₃ values represent the ratio of rate constants for dehydrogenation and cracking; these



Scheme 3. C_3H_8 dehydrocyclodimerization pathways established in reference [44].

Table 7. C_3H_8 dehydrogenation and C_3H_6 cyclodimerization rate constants for H-ZSM5, Ga-ZSM5 and Re^0 -ZSM5 (773 K; 20 kPa C_3H_8).

Catalyst ^[a]	M/Al _f	k_1 ^[b,e]	k_2 ^[c,e]	k_3 ^[d,e]	k_1/k_3 ratio
H	–	0.66	23	1.5	0.44
Ga	0.09	4.2	156	1.9	2.2
Re	0.08	11.0	100	3.6	3.1
Re	0.22	38.4	143	2.5	15.5
Re	0.44	14.1	176	1.6	8.8

[a] Conversions and selectivities given in Table 6. [b] C_3H_8 dehydrogenation rate constant, $r_1 = k_1[C_3H_8]$. [c] C_3H_6 cyclodimerization rate constant, $r_2 = k_2[C_3H_6]$. [d] C_3H_8 cracking rate constant, $r_3 = k_3[C_3H_8]$. [e] [$10^{-1} \text{ L mol}(\text{Al}_f)^{-1} \text{ s}^{-1}$].

ratios are 1.5 times larger for Re^0 -ZSM5 than for Ga-ZSM5 samples ($M/\text{Al} \approx 0.1$). C_3H_8 cyclodimerization constants (k_2) reflect the density and reactivity of residual acid sites combined with the ability of these active sites to remove hydrogen formed in the dehydrogenation steps required to form arenes;^[48] measured k_2 values are in the range of $(100\text{--}180) \times 10^{-1} \text{ L mol}(\text{Al}_f)^{-1} \text{ s}^{-1}$ for all Ga- and Re^0 -ZSM5 catalysts. The value of k_2 was higher for Ga-ZSM5 than for Re^0 -ZSM5 samples that had similar metal loading, regardless of the larger k_1 values on Re^0 -ZSM5. Exchanged cations in ZSM-5 have been shown to increase dehydrocyclization rates by providing sites for the recombinative desorption of H^* surface species.^[48]

The conversion of CH_4 to benzene on Re -ZSM5 has also been reported.^[4] Here, we report CH_4 reaction rates as a function of the Re/Al ratio and compare them with those on Mo-ZSM5 and W-ZSM5 catalysts by using similar reaction conditions. The combined conversion of CH_4 to ethane, ethene, naphthalene, and benzene was limited to 12% by the thermodynamics of the relevant reactions at 950 K (91 kPa CH_4);^[49] therefore, we have corrected net rates for their approach to equilibrium^[50] and report kinetically relevant rates for the forward reaction.

Benzene forward rates and carbon selectivities for CH_4 conversion levels (2.4 and 3.6%) were obtained by using samples of Re -ZSM5 from this study and samples of Mo-ZSM5 and W-ZSM5 reported elsewhere^[4,37,51] (Table 8). The Re -ZSM5 samples in this study gave the highest benzene forward rates among these catalysts (3.7×10^{-3} and $4.1 \times 10^{-3} \text{ mol mol}(\text{Re})^{-1} \text{ s}^{-1}$ for Re/Al_f ratios of 0.22 and 0.08, respectively); specifically, these rates exceed those measured on Mo_2C -ZSM5, which is widely regarded as the most active and selective catalyst for CH_4 pyrolysis.^[52] Re -ZSM5 in this study also showed similar stability to Mo-ZSM5.^[53]

Table 8. CH_4 pyrolysis over M-ZSM5 (M = metal).^[a]

Catalyst	M/Al _f	T [K]	Benzene forward rate [$10^{-3} \text{ mol mol}(\text{M})^{-1} \text{ s}^{-1}$]	Carbon selectivity [%]		
				C ₂	C ₆ –C ₁₁	C ₁₂₊
Re ^[b]	0.08	950	4.1	8	53	35
Re ^[b]	0.22	950	3.7	11	50	31
W ^[b,e]	0.25	973	0.8	16	53	28
Mo ^[b,d]	0.25	950	3.0	13	57	26

[a] Re catalysts were prereduced in H_2/He (5 kPa) at 723 K prior to CH_4 reaction. [b] $\text{Si}/\text{Al}_f = 13.4$, CH_4 (91 kPa), CH_4 ($0.19 \text{ cm}^3 \text{ g}(\text{catalyst})^{-1} \text{ s}^{-1}$). Selectivities reported for CH_4 conversions are between 2.4 and 3.6%. [c] From ref. [51]. [d] From ref. [37].

The first-order deactivation rate constants for benzene were 0.015 ks^{-1} for Re -ZSM5 ($Re/\text{Al}_f = 0.22$) and 0.014 ks^{-1} for Mo-ZSM5 ($Mo/\text{Al}_f = 0.4$).

The similar C_6H_6 formation forward rates reported here on samples with Re/Al_f ratios of 0.22 and 0.08 are consistent with the similar size of Re metal clusters in these two catalysts. The high rates, relative to those in previous reports, indicate that the synthetic protocols reported herein lead to a larger fraction of Re atoms at cluster surfaces, which consequently benefits catalyst productivity. Finally, the excellent stability of these materials during reactions of propane and methane at high temperatures indicates that encapsulation, within the ten-ring zeolite channels in H-ZSM5, can be used to protect Re-metal clusters against agglomeration and inhibit the formation of unreactive organic residues during catalysis.

Conclusions

Synthetic protocols involving the sublimation of Re_2O_7 to prepare isolated and stable $\text{Si-O}_f\text{ReO}_3\text{-Al}$ species on H-ZSM5 are described here. The structure and reactivity of these species is independent of the Re density below a Re/Al_f ratio of 0.44. Their structures were determined by means of infrared, Raman, and extended X-ray-absorption fine-structure spectroscopies. These samples contain $\text{Si-O}_f\text{ReO}_3\text{-Al}$ monomers with Re centers similar in structure to tetrahedral ReO_4^- anions and contain three Re-O bonds (1.7 Å) and one Re-O_f bond (1.8 Å). The oxygen stoichiometry and oxidation state was confirmed by H_2 reduction, which removed three oxygen atoms as H_2O during reduction, while consuming 3.5 H_2 molecules per Re atom. ReO_x -ZSM5 catalyzes C_2H_5OH oxidation reactions at much lower temperatures than those of previously reported Re-based catalysts; the isolated and grafted nature of these active ReO_x species eliminates the ubiquitous sublimation of Re oxides at high temperatures, which has precluded the practical use of ReO_x -based materials in oxidation catalysis. ReO_x -ZSM5 also catalyzed the oxidative conversion of C_2H_5OH at 373 K to $\text{CH}_3\text{CH}_2\text{OCOCH}_3$ and $(\text{CH}_3\text{CH}_2\text{O})_2\text{CHCH}_3$ with only trace formation of total oxidation products. Treatment with H_2 at 723 K reduces $\text{Si-O}_f\text{ReO}_3\text{-Al}$ to form Re^0 clusters $\approx 8.2 \text{ Å}$ in diameter. These encapsulated clusters showed un-

precedented reactivity in the nonoxidative conversion of C_1 and C_3 alkanes to arenes.

Experimental Section

Synthesis of exchanged Re–ZSM5: NH_4 –ZSM5 (7–8 g batches; AlSiPenta, Si/Al₁=13.4; <0.03% wtNa) was treated with a flow of dry air ($1.67\text{ cm}^3\text{ s}^{-1}\text{ g}^{-1}$, Airgas, 99.999%) at 623 K (0.05 K s^{-1} heating rate) for 3 h. The sample was then heated in dry air to 773 K (0.017 K s^{-1}) and held for 5 h to yield H–ZSM5. H–ZSM5 and crystalline Re_2O_7 were treated separately in vacuum at 573 K and 423 K, respectively, to remove adsorbed H_2O (which can interfere with exchange processes and with the spectroscopic and chemical assessments of structure). Re_2O_7 (Aldrich, 99.9+%) was mixed with H–ZSM5 in stagnant N_2 by using an agate mortar and pestle and ground for ≈ 0.1 h to form intimate physical composites (Re/Al₁ ratios between 0.08 and 0.44). Mixtures (0.2 g) were then placed within a fritted U-tube quartz reactor, heated to 723 K (0.167 K s^{-1}) in 20% O_2/He ($0.67\text{ cm}^3\text{ s}^{-1}$, Matheson, 99.999%), and held for 1 h.

Ga–ZSM5 was prepared by using established methods for incipient wetness impregnation of H–ZSM5 with a 0.1 M aqueous $Ga(NO_3)_3$ and treatment in dry air at 773 K for 1 h and in 5 kPa H_2/He at 773 K for 1 h before C_3H_8 reactions.^[54]

Raman and infrared spectroscopy: H–ZSM5 samples were exposed to UV light at ambient temperature, a procedure that led to the removal of unsaturated adsorbed organics, which fluoresce strongly and decrease the quality of Raman spectra.^[16] H–ZSM5 was then physically mixed with Re_2O_7 , pressed into self-supporting wafers, and rotated at ≈ 7 Hz during the acquisition of Raman spectra to minimize laser heating. Wafers were heated to 823 K (0.17 K s^{-1}) for 1 h in dry air and cooled to ambient temperature before measuring Raman spectra by using a HoloLab 5000 Research Raman spectrometer (Kaiser Optical Systems) equipped with a 532 nm laser. Re_2O_7 (Aldrich, 99.9+%), NH_4ReO_4 (Aldrich, 99+%), and aqueous NH_4ReO_4 (0.1 M) solutions were used as Re standards. H–ZSM5 spectra were subtracted from those of Re_2O_7/H –ZSM5 mixtures to measure the vibrational spectra of the ReO_x structures.

Transmission infrared spectra were measured with a Mattson Research Series 10000 FTIR spectrometer. Samples were pressed into wafers (15 mg cm^{-2}) and placed into a cell that has CaF_2 windows. Samples were treated in dry air (Praxair, 99.999%) at 673 K for 0.5 h to remove adsorbed water and the spectra were measured at 673 K by means of 1000 scans between $\tilde{\nu}=1000$ – 4000 cm^{-1} . The intensities of O–H stretching bands ($\tilde{\nu}=3500$ – 3800 cm^{-1}) were normalized to those for the framework Si–O–Si overtone bands ($\tilde{\nu}=1750$ – 2100 cm^{-1}).

X-ray absorption spectroscopy: X-ray absorption spectra were measured by using beamlines 2.3 and 6.2 at the Stanford Synchrotron Radiation Laboratory by using apparatus and protocols described previously^[55] and again briefly below. Samples were pressed into pellets (0.12–0.25 mm) and placed within a quartz capillary (0.8 mm i.d.; 0.1 mm walls) heated by a finned copper block. Spectra were measured in transmission mode by using three ionization chambers filled with N_2 for the Re L_{III} -edge (10.535 keV) or with Ar for the Re L_I -edge (12.527 keV). Detectors were detuned to 50% of maximum intensity to minimize higher harmonics. The capillary was placed between the first and second detector. Re powder (Aldrich, 99.9+%) mixed with boron nitride and held by Kapton tape was placed between the second and third detectors to calibrate the photon energies.

Spectral backgrounds were subtracted from extended X-ray absorption fine-structure (EXAFS) spectra by using WinXAS 2.1.^[56] EXAFS spectra were generated by Fourier transform (between 2 and 13 \AA^{-1}). The k^3 -weighted spectra were then back-transformed (between 1 and 2 \AA or 1 and 3 \AA for Re–ZSM5 treated with 5% H_2/He) and fit by varying coordination number (CN), interatomic distances (R), edge-energy shifts (ΔE_0 , the E_0 difference between Re–ZSM5 and reference standard), and Debye–Waller factors ($\Delta(\sigma^2)$, the σ^2 difference between Re–ZSM5 and reference standard). Backscattering amplitudes and phase-shifts for Re–

Re and Re–O paths were calculated by using the experimental spectra of Re powder (Aldrich, 99.9+%) and NH_4ReO_4 (Aldrich, 99+%), respectively, by means of WinXAS 2.1.

Near-edge spectra at the Re L_I -edge were analyzed by using methods described by Fröba et al.^[57] Spectra were analyzed (12.50–12.62 keV) by using regression algorithms that gave best fits for peak height, position, and full-width at half-height by using 2–3 Gaussian and one arctangent functions. Peak intensities were calculated by multiplying the peak height by this width at half-maximum. Near-edge Re– L_{III} spectra were measured at 0.7 ks intervals during temperature ramping (from 298 to 723 K, 0.05 K s^{-1}) in H_2/He (4 kPa).

Reduction dynamics of ReO_x –ZSM5 in H_2 : The Re–ZSM5 samples (0.05–0.2 g) that were prepared following the procedures described above were dehydrated at 723 K in 20% O_2/He ($1\text{ cm}^3\text{ s}^{-1}$, Matheson, 99.999%) for 1 h and then cooled to ambient temperature in He ($1\text{ cm}^3\text{ s}^{-1}$, Praxair, 99.999%) before H_2 treatment. The flow was then changed to a H_2/He mixture ($1\text{ cm}^3\text{ s}^{-1}$, 4 kPa, Praxair, 99.999%) and heated to 723 K (0.167 K s^{-1}). The effluent stream was analyzed by using mass spectrometry (MKS Minilab) by means of transfer lines kept at 423 K. Response factors for H_2 (2 amu) and H_2O (18 amu) were determined by stoichiometric reduction of CuO powders by using a He (4 amu) internal standard.

Nonoxidative catalytic conversion of propane and methane to aromatics: Re–ZSM5 materials (0.1–0.2 g) were treated in H_2/He (4 kPa, Praxair, 99.999%) as described above, and then exposed to C_3H_8 (Praxair, 20 kPa, Research Purity), Ar (5 kPa 99.999%), and He (75 kPa 99.999%) at 773 K within a fritted quartz reactor (8 mm diameter). Reactant and product concentrations in the effluent stream were measured by using gas chromatography (Agilent 6890) by direct transfer through transfer lines kept at 450 K. Hydrocarbons were separated by using a capillary column (Agilent HP-1, $50\text{ m}\times 0.32\text{ mm}\times 1.05\text{ }\mu\text{m}$ film) and detected by means of flame ionization. C_2H_6 , H_2 , and Ar were separated by using a packed column (Agilent Poropak Q, 4.5 m) and detected by means of thermal conductivity. C_3H_8 conversions were measured by using Ar as an internal standard. Product selectivities are defined as the percentage of the C_3H_8 converted appearing as each product. CH_4 reactions were carried out at 950 K and in CH_4 (91 kPa) with Ar (Praxair, 99.999%) as a balance gas at ambient pressure after treating catalyst samples (0.5 g) in H_2/He (4 kPa) to 723 K (0.17 K s^{-1}) for 1 h. Reactant conversion and product selectivity were measured as in the case of propane reactants.

Catalytic ethanol-oxidation reactions: C_2H_5OH reaction rates and selectivities were measured at 373 K in C_2H_5OH (4 kPa), O_2 (9 kPa), and pressure balanced with He ($464\text{ cm}^3\text{ g(Re)}^{-1}\text{ s}^{-1}$) on Re–ZSM5 (0.1 g) diluted with quartz (1 g; washed in concentrated aqueous HNO_3 and treated in dry air at 773 K). Effluent concentrations were measured by using gas chromatography (Agilent 6890) by direct transfer from the reactor outlet through transfer lines kept at 450 K. Hydrocarbons were separated by using a capillary column (Agilent HP-1, $50\text{ m}\times 0.32\text{ mm}\times 1.05\text{ }\mu\text{m}$ film) and detected by using flame ionization, and CO and CO_2 were separated in a packed column (Agilent Poropak Q, 80–100 mesh, $1.8\text{ m}\times 3.2\text{ mm}$) and detected by means of thermal conductivity. Selectivities of products are defined as the fraction of C_2H_5OH converted appearing as each product. Oxidative-dehydrogenation (ODH) rates were obtained from measured CH_3CHO (acetaldehyde), $CH_3CH_2OCOCH_3$ (ethyl acetate), and $(CH_3CH_2O)_2CHCH_3$ (acetal) rates by assuming that each mole of product required the conversion of one C_2H_5OH molecule to acetaldehyde; the latter has been shown to act as an intermediate in the formation of ethyl acetate and acetal.^[40]

Acknowledgements

This research was funded in part by BP through the Berkeley-Caltech Methane Conversion Cooperative Program. H.L. acknowledges the Ford Foundation for a fellowship granted through the Berkeley Catalysis

Center. X-ray absorption spectra were measured at the Stanford Synchrotron Radiation Laboratory, a national user facility operated by Stanford University on behalf of the U.S. Department of Energy, Office of Basic Energy Sciences.

- [1] J. A. Moulijn, J. C. Mol, *J. Mol. Catal. A: Chem.* **1988**, *46*, 1.
[2] J. C. Mol, *Catal. Today* **1999**, *51*, 289.
[3] W. Daniell, T. Weingand, H. Knözinger, *J. Mol. Catal. A* **2003**, *204*, 519.
[4] L. Wang, R. Ohnishi, M. Ichikawa, *J. Catal.* **2000**, *190*, 276.
[5] R. Bal, M. Tada, T. Sasaki, Y. Iwasawa, *Angew. Chem.* **2006**, *118*, 462; *Angew. Chem. Int. Ed.* **2006**, *45*, 448.
[6] N. Viswanadham, T. Shido, Y. Iwasawa, *Appl. Catal. A* **2001**, *219*, 223.
[7] N. Viswanadham, T. Shido, T. Sasaki, Y. Iwasawa, *Sci. Tech. Catal.* **2002**, *35*, 189.
[8] N. Viswanadham, T. Shido, T. Sasaki, Y. Iwasawa, *J. Phys. Chem. B* **2002**, *106*, 10955.
[9] L. Wang, R. Ohnishi, M. Ichikawa, *Catal. Lett.* **1999**, *62*, 29.
[10] Y. Shu, R. Ohnishi, M. Ichikawa, *Appl. Catal. A* **2003**, *252*, 315.
[11] Y. Shu, M. Ichikawa, *Catal. Today* **2001**, *71*, 55.
[12] F. Solymosi, P. Tolmascov, *Catal. Lett.* **2004**, *93*, 7.
[13] F. Solymosi, P. Tolmascov, A. Széchenyi, *Stud. Surf. Sci. Catal.* **2004**, *147*, 559.
[14] D. R. Lide, *CRC Handbook of Chemistry and Physics*, 75th ed., CRC Press, Boca Raton, **1994**.
[15] O. Knacke, O. Kubaschewski, K. Hesselmann, *Thermochemical Properties of Inorganic Substances*, 2nd ed., Springer-Verlag, Berlin, **1991**.
[16] H. S. Lacheen, P. J. Cordeiro, E. Iglesia, *J. Am. Chem. Soc.* **2006**, *128*, 15082.
[17] Y.-H. Kim, R. W. Borry, E. Iglesia, *Microporous Mesoporous Mater.* **2000**, *35*, 495.
[18] W. Li, G. D. Meitzner, R. W. Borry, E. Iglesia, *J. Catal.* **2000**, *191*, 373.
[19] H. Liu, E. Iglesia, *J. Phys. Chem. B* **2003**, *107*, 10840.
[20] J. R. Mowry, R. F. Anderson, J. A. Johnson, *Oil Gas J.* **1985**, *83*, 128.
[21] G. L. Price, V. I. Kanazirev, *J. Catal.* **1990**, *126*, 267.
[22] B. Krebs, A. Müller, H. H. Beyer, *Chem. Commun.(London)* **1968**, *5*, 263.
[23] F. D. Hardcastle, I. E. Wachs, J. A. Horsley, G. H. Via, *J. Mol. Catal. A: Chem.* **1988**, *46*, 15.
[24] F. P. J. M. Kerkhof, J. A. Moulijn, R. Thomas, *J. Catal.* **1979**, *56*, 279.
[25] L. A. Woodward, H. L. Roberts, *Trans. Faraday Soc.* **1956**, *52*, 615.
[26] K. Ulbricht, H. Kriegsmann, *Z. Anorg. Allg. Chem.* **1968**, *358*, 193.
[27] K. Ulbricht, H. Kriegsmann, *Z. Chem.* **1966**, *6*, 232.
[28] L. Wang, W. K. Hall, *J. Catal.* **1983**, *82*, 177.
[29] G. J. Kruger, E. C. Reynhardt, *Acta Crystallogr. Sect. B* **1978**, *259*.
[30] Al₂O₃-supported Re⁷⁺-oxo species prepared by impregnation led to smaller shifts of the A1 mode upon exposure to H₂O, apparently due to lower ReO_x dispersion; a) F. D. Hardcastle, I. E. Wachs, J. A. Horsley, G. H. Via, *J. Mol. Catal.* **1988**, *46*, 15; b) L. Wang, W. K. Hall, *J. Catal.* **1983**, *82*, 177.
[31] H. S. Lacheen, E. Iglesia, *J. Phys. Chem. B* **2006**, *110*, 5462.
[32] Features below 0.1 nm are due to low frequency noise and do not represent scattering from a nearby atom.
[33] J. A. Dean, *Langes Handbook of Chemistry*, 14th ed., McGraw-Hill, New York, **1992**.
[34] M. D. Foster, I. Rivin, M. M. J. Treacy, O. Delgado Friedrichs, *Microporous Mesoporous Mater.* **2006**, *90*, 32.
[35] S. Liu, L. Wang, R. Ohnishi, M. Ichikawa, *J. Catal.* **1999**, *181*, 175.
[36] W. Ding, G. D. Meitzner, D. O. Marler, E. Iglesia, *J. Phys. Chem. B* **2001**, *105*, 3928.
[37] H. S. Lacheen, E. Iglesia, *J. Catal.* **2005**, *230*, 173.
[38] R. Ohnishi, S. Liu, Q. Dong, L. Wang, M. Ichikawa, *J. Catal.* **1999**, *182*, 92.
[39] C. J. Machiels, A. W. Sleight, *J. Catal.* **1982**, *76*, 238.
[40] H. Liu, E. Iglesia, *J. Phys. Chem. B* **2005**, *109*, 2155.
[41] Y. Yuan, Y. Iwasawa, *J. Phys. Chem. B* **2002**, *106*, 4441.
[42] W. T. A. Harrison, A. V. P. McManus, M. P. Kaminsky, A. K. Cheetham, *Chem. Mater.* **1993**, *5*, 1631.
[43] W. A. Herrmann, R. W. Fischer, D. W. Marz, *Angew. Chem.* **1991**, *103*, 1706; *Angew. Chem. Int. Ed. Engl.* **1991**, *30*, 1638.
[44] J. A. Biscardi, E. Iglesia, *J. Catal.* **1999**, *182*, 117.
[45] H. Kitagawa, Y. Sendoda, Y. Ono, *J. Catal.* **1986**, *101*, 12.
[46] T. Mole, J. R. Anderson, G. Creer, *Appl. Catal.* **1985**, *17*, 141.
[47] H. Berndt, G. Lietz, B. Lücke, J. Völter, *Appl. Catal. A* **1996**, *146*, 351.
[48] S. Y. Yu, J. A. Biscardi, E. Iglesia, *J. Phys. Chem. B* **2002**, *106*, 9642.
[49] Chemkin Collection Version 3.6, Reaction Design, San Diego, CA, **2000**.
[50] M. Boudart, G. Djega-Mariadassou, *Kinetics of Heterogeneous Catalytic Reactions*, Princeton University Press, Princeton, NJ, **1984**.
[51] H. S. Lacheen, E. Iglesia, *Phys. Chem. Chem. Phys.* **2005**, *7*, 538.
[52] D. Wang, J. H. Lunsford, M. P. Rosynek, *Top. Catal.* **1996**, *3*, 289.
[53] The stability of Re-ZSM5 to coking was examined by running CH₄ reactions for extended periods of time. Catalyst deactivation displayed first-order kinetics, and a rate constant, *k_D*, for deactivation was calculated. Re-ZSM5 had *k_D* values of 0.018 and 0.015 ks⁻¹ for Re/Al_i ratios of 0.1 and 0.22, respectively, and were comparable to Mo- and W-ZSM5 that have a *k_D* of 0.014 and 0.011 ks⁻¹, respectively. Deactivation is assumed to occur through carbon formation on zeolite external surfaces that inhibit access to channel entrances.
[54] P. Mériaudeau, C. Naccache, *Appl. Catal.* **1991**, *73*, L13.
[55] D. G. Barton, S. L. Soled, G. D. Meitzner, G. A. Fuentes, E. Iglesia, *J. Catal.* **1999**, *181*, 57.
[56] T. Ressler, WinXAS Version 2.1, T. Ressler, Fritz Haber Institut, Berlin (Germany).
[57] M. Fröba, K. Lochte, W. Metz, *J. Phys. Chem. Solids* **1996**, *57*, 635.

Received: November 10, 2006
Published online: February 26, 2007